Conjugated Side-Chain Isolated Polythiophene: Synthesis and Photovoltaic Application

ARTICLE *in* MACROMOLECULES · DECEMBER 2011

Impact Factor: 5.8 · DOI: 10.1021/ma201718x

Macromolecules

Article

pubs.acs.org/Macromolecules

Conjugated Side-Chain Isolated Polythiophene: Synthesis and Photovoltaic Application

Zhi-Guo Zhang, Siyuan Zhang, Jie Min, Chaohua Chui, Jing Zhang, Maojie Zhang, and Yongfang Li*

Beijing National Laboratory for Molecular Sciences, CAS Key Laboratory of Organic Solids, Institute of Chemistry, Chinese Academy of Sciences, Beijing 100190, China

Supporting Information

ABSTRACT: A design concept of "side chain isolation" was proposed for developing new polythiophene derivatives with conjugated side chain (CSC-PTs), and **PT5TPA** with styryl−triphenylamine (TPA) side chain and unsubstituted tetrathienyl spacer was designed and synthesized. Compared to previously reported CSC-PTs, side chain isolated **PT5TPA** showed red-shifted and enhanced $\pi-\pi^*$ transition absorption of the polymer backbone along with the shoulder peak and steep absorption edge, indicating improved planarity of the backbone. In addition, the unsubstituted thiophene spacer along the polymer backbone of the side chain isolated **PT5TPA** results in a lower HOMO energy level of the polymer at −5.1 eV. The polymer solar cell based on **PT5TPA** as donor and indene−C_{60} bisadduct as acceptor displayed a power conversion efficiency of 3.6% with a high open circuit voltage of 0.94 V, under the illumination of AM1.5G, 100 mW/cm^2. The results indicate that the side chain isolated CSC-PTs could open a new way for developing high performance photovoltaic polymers.

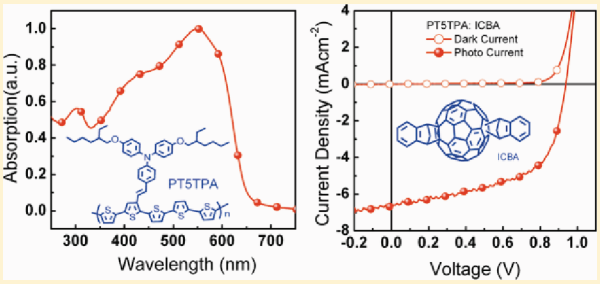

1. INTRODUCTION

Bulk heterojunction (BHJ) polymer solar cells (PSCs) based on *p*-type conjugated polymers as donor[1,2] and *n*-type fullerene[3,4] as acceptor have been intensively studied in recent years for the generation of affordable, clean, and renewable energy.[5] Advantages of the BHJ PSCs include low-cost fabrication of large-area devices, light weight, mechanical flexibility, and easy tunability of chemical properties of the photovoltaic materials.[6]

Poly(thiophene) derivatives (PTs) have been among the most extensively investigated conjugated polymers due to their high charge carrier mobility, strong absorption in visible region and synthetic accessibility.[7−12] Soluble poly(3-alkylthiophene)s, especially regioregular poly(3-hexylthiophene) (P3HT), are the most important semiconducting polymers for the application in PSCs.[9−12] However, the power conversion efficiency (PCE) of the PSCs based on P3HT as donor and PCBM as acceptor is limited at 4−5%,[13,14] because of its larger band gap and its high HOMO (the highest occupied molecular orbital) energy level, which result in limited light absorption and a low open circuit voltage (V_{oc}) of the PSCs. In addition, the high regioregularity-induced crystallization may be an issue of thermal instability of the blend of P3HT and fullerene acceptors.

For broadening the absorption of the PTs, the polythiophene derivatives with conjugated side chain (CSC-PTs, where CSC represents "conjugated side chain") were designed and synthesized in our group.[15−17] The CSC-PTs possess 2-D charge transport properties thanks to the 2-D-conjugated character of the polymer structure, and broad absorptions deriving from both the main chains and conjugated side chains; thus, this family of CSC-PTs demonstrated good device performances in PSCs[15a] and organic field-effect transistors (OFETs).[16] However, due to steric hindrance of the large conjugated side chain with other alkyl side chains on the polymer main chain, the CSC-PTs showed poorer planarity, which is detrimental for the close packing of polymer chains in the solid state, as clearly evidenced for the featureless absorption along with the low absorption intensity of $\pi-\pi^*$ absorption.[15−17] As a result, this structural limitation constrains their application in organic electronics and the highest PCE value of the CSC-PTs reported so far was 3.18%.[15a] To further improve the optical properties, creating the CSC-PTs without scarifying the planarity/conjugation of the thiophene backbone is very desirable. Fulfilling this goal presents serious challenges in chemistry.

To address this issue, here we proposed the "side chain isolation" concept in designing the new CSC-PTs. We selected styryl−triphenylamine (TPA) as the conjugated side chain in considering the high hole mobility and good solubility of the TPA unit, and we used a tetrathiophene unit without side chains as the spacer between the thiophene units with the conjugated side chains for avoiding the steric hindrance of the side chains. In addition, two 2-ethylhexyloxyl groups were directly attached at the terminal of the TPA side chains to

Received: July 25, 2011
Revised: November 23, 2011
Published: December 6, 2011

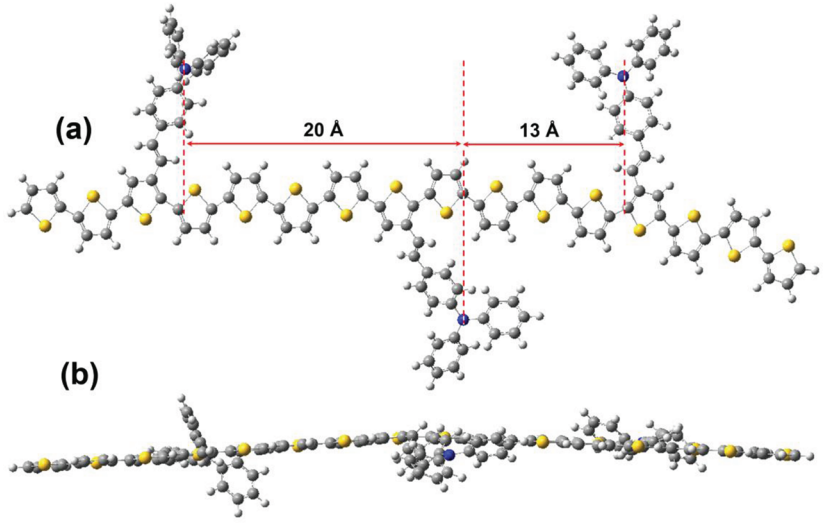

Figure 1. Optimized geometry of PT5TPA: (a) top view and (b) side view.

Scheme 1. Synthesis Route of PT5TPA

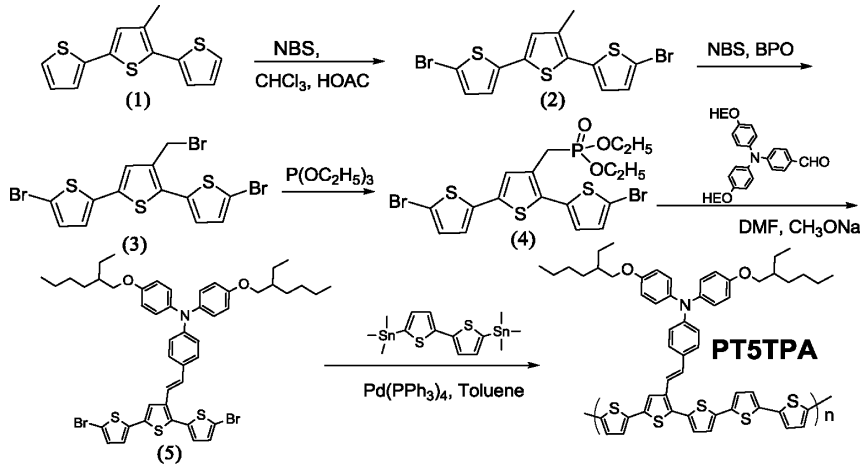

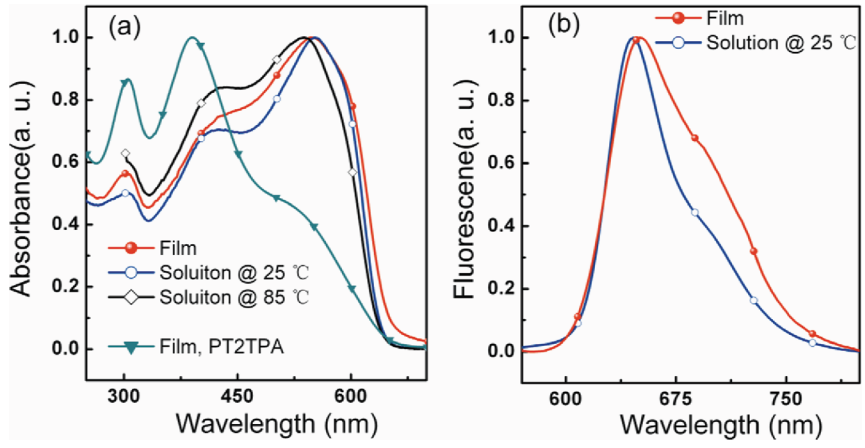

Figure 2. (a) Absorption spectra of PT5TPA in film and in dichlorobenzene solution (at room temperature and high temperature of 85 °C) and the absorption spectrum of PT2TPA film for comparison. (b) PL spectra of PT5TPA in film and dichlorobenzene solution, excited at 430 nm.

ensure good solubility. According to the molecular mechanics simulation (performed with COMPASS force field within the Materials Studio Package[18]) as shown in Figure 1, the side-chains of **PT5TPA** oriented in the tail-to-tail direction are spaced approximately 13 Å apart while those side chains orientated in the head-to-tail fashions are 20 Å apart. Thus, this side chain isolation approach combines the thiophene units bearing conjugated side chain and the unsubstituted tetrathienyl spacers to reduce the steric interactions between the neighbor side chains, which lessens the torsion of the main

dx.doi.org/10.1021/ma201718x | *Macromolecules* 2012, 45, 113–118

chains (see Figure 1b). This CSC-PT of **PT5TPA** demonstrated red-shifted and enhanced $\pi-\pi^*$ transition absorption of the polymer backbone along with the shoulder peak and steep absorption edge, indicating some ordered aggregation of the polymer backbone. In addition, the polymer shows a lower HOMO energy level at −5.1 eV. The PSC based on **PT5TPA** as donor and indene−C_{60} bisadduct ($IC_{60}BA$)[4] as acceptor displayed a PCE of 3.6% with a high open circuit voltage of 0.94 V, under the illumination of AM1.5G, 100 mW/cm^2.

2. RESULTS AND DISCUSSION

Polymer Synthesis and Characterizations. Chemical structure and synthetic route of **PT5TPA** with TPA−vinylene conjugated side chain are depicted in Schemes 1. Bromination of compound **1** with *N*-bromosuccinimide (NBS), performed initially in chloroform at room temperature, and subsequently in anhydrous carbon tetrachloride with benzoyl peroxide (BPO) as catalyst, yielded product **3** with bromomethyl functionality. A Michaelis−Arbuzov reaction[19] was performed between compound **3** with triethyl phosphate afford phosphonate precursor **4**, which was transferred to dibromide monomer **5** via a Horner−Wordsworth−Emmons (HWE) reaction.[20] The polymer was synthesized by palladium(0)-catalyzed Stille polycondensation[21] of an equimolecular mixture of the dibromide and distannyl bithiophene. The polymer is soluble in chlorinated solvents, such as chloroform, chlorobenzene and dichlorobenzene, and exhibited a number-average molecular weight (M_n) of 180.9 K, with a polydispersity index of 3.2. Thermogravimetric analysis (TGA), as shown in Figure S1 in Supporting Information (SI), demonstrated a good thermal stability of the polymer with a 5% weight-loss temperature at 354 °C. DSC was measured in the temperature range of 30−280 °C, but we did not find the glass transition temperature in the temperature range. (see Figure S2 in Supporting Information).

Optical and Electrochemical Properties. Figure 2a shows the absorption spectra of PT5TPA solution in chloroform and film on quartz plate, together with the absorption spectrum of **PT2TPA** film[16a] (**PT2TPA** is a **PT5TPA**-analogue polymer with only one thiophene spacer, named as OTPAV-PT in ref 16a). The solution and film absorption of **PT5TPA** display similar broad absorption band from 300 to 650 nm with three distinct absorption peaks. The two weak absorption peaks around 303 and 413 nm originate respectively from n−π^* transition of TPA group[22] and the absorption of the thiophene units with the conjugated side chain, while the maximum absorption of the copolymer at 555 nm corresponds to the $\pi-\pi^*$ transition of the polymer backbone. Thus, both the main chain and side chain contribute to the broad nature of the absorption spectra of the polymer, which is a common feature for PTs with conjugated side chains.[15,16] Because of an enlarged π-system, the film absorption of **PT5TPA** is red-shifted by ca. 10 nm than that of P3HT. The absorption edge of the polymer film is at 658 nm, corresponding to an optical band gap of 1.88 eV. The similarity of solution absorption to film absorption suggests strong $\pi-\pi$ interactions (aggregation) in solution. As shown in Figure 2a, when the polymer solution was heated to 85 °C, the absorption peaks blue shift, and the shoulder peak at ca. 600 nm weakened, reflecting partial disaggregation of the polymer backbone at high temperature. Also it must mention that the obtained high molecular weight of **PT5TPA** could be overestimated due to the easily formed polymer aggregation state at room temperature.

In comparison with the absorption spectrum of **PT2TPA** film[16a] as also shown in Figure 2a, the $\pi-\pi^*$ absorption of PT5TPA main chains at ca. 500−650 nm is greatly enhanced than that of the CSC-PTs with concentrated side chains.[15−17] Obviously, the side chain isolated **PT5TPA** can minimize the steric interactions between the neighboring side chains, thus preserving backbone planarity, which results in the red-shifted and enhanced $\pi-\pi^*$ transition of the polymer backbone along with the shoulder peak and steep absorption edge. Furthermore, the well-defined spectra of PT5TPA imply an ordered polymer chains and densely packed side chains in the polymer film, which should benefit to higher hole mobility and photovoltaic performance of the polymer. In order to further investigate the ordered structure of the polymer, we measured X-ray diffraction (XRD) of the polymer film on Si substrate. The XRD pattern of the polymer film (see Figure S7 in Supporting Information) indicates that the polymer film is still in amorphous state although the aggregation is enhanced in the polymer. The hole mobility of PT5TPA film was measured to be 1.1 × 10^{-3} cm^2/(V s) by space charge limited current (SCLC) method (see Figure S3 in Supporting Information), confirming the relatively higher hole mobility of the polymer.

Figure 2b shows the photoluminescence (PL) spectra of **PT5TPA** solution in dichlorobenzene and film, excited at 430 nm, which is the maximum absorption wavelength of the conjugated side chains of the polymer. **PT5TPA** shows deep red main chain emission peaked at 670 nm. The results indicate that quick and complete energy transfer occurs from the conjugated side chains to the polymer main chains after the conjugated side chains absorb the photons. This phenomenon ensures that all photons absorbed by the polymer are useful for the photovoltaic conversion.

The electronic energy levels of the conjugated polymers can be measured from the onset oxidation and onset reduction potentials of the cyclic voltammograms (CVs).[23] Figure 3 shows the cyclic voltammogram of **PT5TPA** together with that of P3HT for comparison and that of ferrocene for potential calibration. The redox potential of ferrocene is 0.09 V vs Ag/Ag$^+$. On the basis of 4.8 eV below vacuum for the energy level of Fc/Fc$^+$, the HOMO and LUMO energy levels of PT5TPA were calculated according to the following equations: $E_{HOMO} = -e(E_{ox}^{onset}+4.71)$ (eV) and $E_{LUMO} = -e(E_{red}^{onset}+4.71)$, where

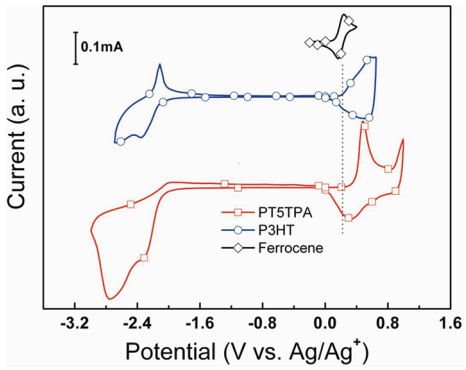

Figure 3. Cyclic voltammograms of PT5TPA and P3HT films on glassy carbon electrode in a 0.1 mol/L *n*-Bu_4NPF_6 acetonitrile solution at a sweep rate of 100 mV/s. The cyclic voltammogram of ferrocene was also put in the figure for the potential calibration.

dx.doi.org/10.1021/ma201718x | *Macromolecules* 2012, 45, 113−118

the unit of E_{ox}^{onset} is V vs. Ag/Ag^+. The onset oxidation potential (E_{ox}^{onset}) and onset reduction potential (E_{red}^{onset}) of **PT5TPA** are 0.39 and −1.63 V vs. Ag/Ag^+ respectively, accordingly, the HOMO and LUMO energy levels of PT5TPA were calculated to be −5.10 and −3.08 eV respectively. Compared to that of P3HT, the onset oxidation potential of **PT5TPA** is positively shifted by ca. 0.2 V and the HOMO energy level of **PT5TPA** is downward shifted by ca. 0.2 eV, which is due to less alkyl substituents of **PT5TPA** than that of P3HT.[12b] The lower HOMO energy level relative to P3HT can provide better air stability in ambient conditions and higher open circuit voltage (V_{oc}) of the PSCs with **PT5TPA** as donor materials because the V_{oc} is usually proportional to the difference between the LUMO level of the acceptor and the HOMO level of the donor.[6]

Photovoltaic Properties. The photovoltaic properties of **PT5TPA** were studied by fabricating the bulk heterojunction PSCs with the device configuration of ITO/PEDOT:PSS/PT5TPA:acceptors/Ca/Al. Here, two different fullerene derivatives $PC_{70}BM$ and $IC_{60}BA$ were used as acceptor in the PSCs. The molecular structures and the electronic energy level diagrams of the donor and acceptor materials were displayed in Figure 4. Figure 5 shows the $J-V$ curves of the PSCs based on

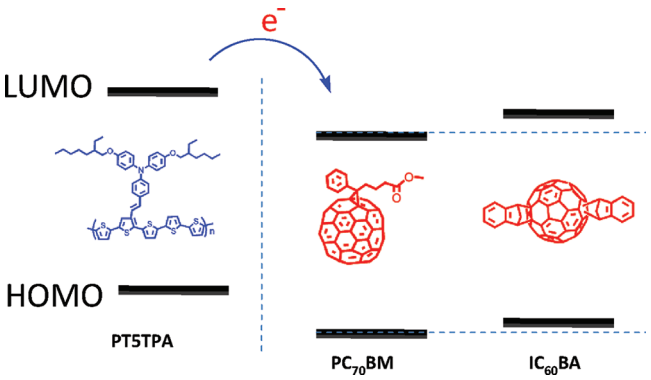

Figure 4. Energy level diagrams for PT5TPA along with acceptors of $PC_{70}BM$ and $IC_{60}BA$.

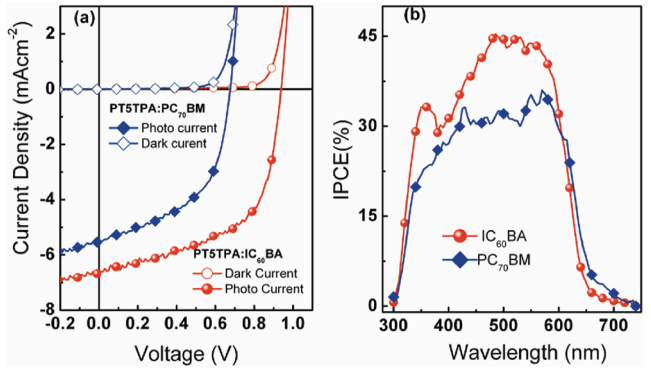

Figure 5. (a) Current density−voltage characteristics of the PSCs based on PT5TPA/fullerene (1:1, w/w) under the illumination of AM1.5G, 100 mW/cm^2. (b) The incident-photon-to-converted-current efficiency (IPCE) spectra of the corresponding devices with different fullerene acceptors.

PT5TPA as donor and $PC_{70}BM$ or $IC_{60}BA$ as acceptor under the illumination of AM 1.5, 100 mW·cm^{-2}. With the widely used $PC_{70}BM$ as acceptor, the PSC showed a PCE of 1.94% along with a V_{oc} of 0.68 V and a FF of 52.2%, while when using $IC_{60}BA$ as acceptor, a higher V_{oc} of 0.94 V was obtained, benefitted from the higher-lying LUMO energy level of $IC_{60}BA$.[4] Together with a J_{sc} of 6.55 mA cm^{-2} and a FF of 58.4%, the PSC based on PT5TPA/$IC_{60}BA$ demonstrated an improved PCE of 3.6%. Although the PCE of 3.6% is lower than that of the PSC based on P3HT/$IC_{60}BA$,[4] it is the highest value reported so far for the CSC-PTs. In the PSCs based on PT5TPA, the FF values (Table 1) are significantly improved in comparison with the CSC-PTs with concentrated side chains,[15,16,17f,24] which could be ascribed to the close aggregation of the polymer main chains in the side chain isolated polymers.

Table 1. Photovoltaic Parameters of PSCs Based on PT5TPA as Donor and $PC_{70}BM$ or $IC_{60}BA$ as Acceptor, under the Illumination of AM1.5G, 100 mW/cm^2

acceptors	weight ratio	V_{oc} (V)	J_{sc} (mAcm^{-2})	FF (%)	PCE (%)	active layer thickness (nm)
$PC_{70}BM$	1:1	0.68	5.46	52.2	1.94	65
$IC_{60}BA$	1:1	0.94	6.55	58.4	3.60	70

3. CONCLUSION

A design concept of "side chain isolation" was proposed for CSC-PTs, and a planar CSC-PT, **PT5TPA**, with styryl−triphenylamine (TPA) side chains and unsubstituted tetrathienyl spacer was designed and synthesized. Compared to previously reported CSC-PTs, side chain isolated **PT5TPA** demonstrated the red-shifted and enhanced $\pi-\pi^*$ transition absorption of the polymer backbone along with the shoulder peak and steep absorption edge. In addition, the unsubstituted thiophene spacer lead the polymer a lower HOMO energy level of −5.1 eV. The PSC based on **PT5TPA** as donor and $IC_{60}BA$ as acceptor displayed a PCE of 3.6% with a high V_{oc} of 0.94 V, under the illumination of AM1.5G, 100 mW/cm^2.

Considering the diversity molecular engineering approach under this side chain isolated polythiophenes, such as changing the nature of side chain and spacer as well as introducing D−A concept, the side chain isolated CSC-PTs could open a new way for developing high performance photovoltaic polymers.

4. EXPERIMENTAL SECTION

4.1. Instrumentation. ^{1}H NMR spectra were measured on a Bruker DMX-400 spectrometer with *d*-chloroform as the solvent and tetramethylsilane as the internal reference. UV−visible absorption spectra were measured on a Hitachi U-3010 UV−vis spectrophotometer. MALDI−TOF spectra were recorded on a Bruker BIFLEXIII. Absorption spectra were taken on a Hitachi U-3010 UV−vis spectrophotometer. Photoluminescence spectra were measured using a Hitachi F-4500 spectrophotometer. Mass spectra were recorded on a Shimadzu spectrometer. Elemental analyses were carried out on a flash EA 1112 elemental analyzer. Thermogravimetric analysis (TGA) was conducted on a Perkin-Elmer TGA-7 thermogravimetric analyzer at a heating rate of 20 °C/min and under a nitrogen flow rate of 100 mL/min. Molecular weight of the polymer was measured by Gel permeation chromatography (GPC), using polystyrene as standard and THF as the eluent. The electrochemical cyclic voltammetry was performed on a Zahner IM6e Electrochemical Workstation, in an acetonitrile solution of 0.1 mol/L tetrabutylammonium hexafluorophosphate (n-Bu_4NPF_6) at a potential scan rate of 100 mV/s with an Ag/Ag^+ reference electrode and a platinum wire counter electrode. Polymer film was formed by drop-casting 1.0 mL of polymer solutions in THF (analytical reagent, 1 mg/mL) onto the glassy carbon working electrode, and then dried in the air.

dx.doi.org/10.1021/ma201718x | *Macromolecules* 2012, 45, 113−118

4.2. Photovoltaic Device Fabrication and Characterization. The PSCs were fabricated with a configuration of ITO/PEDOT:PSS (40 nm)/active layer (65−70 nm)/ Ca(20 nm)/Al(90 nm). A thin layer of PEDOT:PSS (poly(3,4-ethylenedioxythiophene): poly(styrenesulfonate)) was spin-cast on pre-cleaned ITO-coated glass from a PEDOT:PSS aqueous solution (Baytron P VP AI 4083 from H. C. Starck) at 2000 rpm and dried subsequently at 150 °C for 30 min in air, then the device was transferred to a glovebox, where the active layer of the blend of the polymer and fullerene derivative was spin-coated onto the PEDOT:PSS layer. Finally, a Ca/Al metal top electrode was deposited in vacuum onto the active layer at a pressure of ca. 5×10^{-5} Pa. The active area of the device was ca. 4 mm^2.

The thickness of the active layer was determined by an Ambios Tech. XP-2 profilometer. The current density−voltage (J−V) characteristics were measured on a computer-controlled Keithley 236 Source-Measure Unit. A xenon lamp coupled with AM 1.5 solar spectrum filter was used as the light source, and the optical power at the sample was 100 mW/cm^2.

4.3. Materials. 3′-Methyl[2,2′,5′,2″]terthiophene,[25] 5,5′-bis(trimethylstannyl)-2,2′-bithiophene[26] and 4-((4-(2-ethylheptyloxy)phenyl)(4-(2-ethylhexyloxy)phenyl)amino)benzaldehyde[27] were prepared according to the method reported in literatures. Tetrakis(triphenylphosphine)palladium, *N*-Bromosuccinimide and benzoyl peroxide were purchased from Sigma-Aldrich Chemical Co. The synthesis routes for the polymer are shown in Scheme 1.

*5,5″-Dibromo-3′-methyl[2,2′,5′,2″]terthiophene (**2**).* *N*-Bromosuccinimide (NBS, 28.5 g, 160 mmol) was added to a solution of 3′-methyl[2, 2′,5′,2″]terthiophene (20.0 g, 76.3 mmol) in $CHCl_3$ (180 mL) and AcOH (100 mL) at room temperature. After stirring for 3 h, $CHCl_3$ was added and the resulting mixture washed three times with water. The organic layer was dried ($MgSO_4$) and concentrated under reduced pressure. The crude product was purified via silica gel column chromatography afford a green solid with a yield of 27.2 g (85%). GC−MS: m/z = 420. ^{1}H NMR (400 MHz, $CDCl_3$, δ, ppm): 7.02 (d, J = 3.8 Hz, 1 H, Ar−H), 6.96 (d, J = 3.8 Hz, 1 H, Ar−H), 6.88 (m, 3H, Ar−H), 2.33 (s, 3H, CH_3). Anal. Calcd for $C_{13}H_8Br_2S_3$: C, 37.16; H, 1.92; S, 22.89. Found: C, 37.10; H, 1.98; S, 22.75.

*5,5″-Dibromo-3′-bromomethyl[2,2′,5′,2″]terthiophene (**3**).* A mixture of compound **2** (21.0 g, 50 mmol), N-bromosuccinimide (NBS) (8.9 g, 50 mmol), CCl_4 (400 mL), and benzoyl peroxide (BPO) (0.15 g, 0.62 mmol) was refluxed for 3 h. After cooling to the room temperature, the reaction mixture was filtrated. The organic phase was washed with distilled water and dried over anhydrous $MgSO_4$. After removing the solvent, the crude product was purified via silica gel column chromatography to yield a yellow product of compound **3**. ^{1}H NMR (400 MHz, $CDCl_3$, δ, ppm): 7.08−7.07 (m, 2H, Ar−H), 7.05 (d, 1H, J = 3.6 Hz, Ar−H), 6.98 (d, 1H, J = 3.5 Hz, Ar−H), 6.92 (d, 1H, J = 3.6 Hz, Ar−H), 4.53 (S, 2H, $-CH_2-$). Anal. Calcd for $C_{13}H_7Br_3S_3$: C, 31.28; H, 1.41; S, 19.27. Found: C, 31.35; H, 1.38; S, 19.19.

*5,5″-Dibromo-3′-diethoxyphosphorylmethyl[2,2′,5′,2″]-terthiophene (**4**).* A mixture of **3** (15.0 g, 30.0 mmol) and triethyl phosphate (16.6 g, 100.0 mmol) was heated at 160 °C for 3 h. After cooling to room temperature, the triethyl phosphite was distilled off at 120 °C. After removing the solvent, the crude product was purified via silica gel column chromatography to yield a liquid of 15 g (90%). ^{1}H NMR (400 MHz, $CDCl_3$, δ, ppm): 7.13 (s, 1H, ArH), 7.06 (d, J = 4.0 Hz, 1H, ArH), 7.04 (d, J = 4.0 Hz, 1H, ArH), 6.96 (d, J = 3.6 Hz, 1H, ArH), 6.90 (d, J = 3.6 Hz, 1H, ArH), 4.0 (q, 4H, OCH_2), 3.22 (d, J = 20 Hz, 2H, CH_2), 4.0 (t, 6H, CH_3). Anal. Calcd for $C_{17}H_{17}Br_2O_3PS_3$: C, 36.70; H, 3.08; S, 17.29. Found: C, 36.63; H, 3.00; S, 17.32.

*5,5″-Dibromo-3′,3-(4-((4-(2-ethylheptyloxy)phenyl)(4-(2-ethylhexyloxy)phenyl)amino)benzvinyl[2,2′,5′,2″]terthiophene (**5**).* Under an ice−water bath, compound **4** (5.56 g, 10 mmol) and aldehyde (6.50 g, 12 mmol) were dissolved in 30 mL of DMF, and then CH_3ONa (0.6 g, 12 mmol) in 10 mL of DMF was added dropwise to the solution. After reaction for 2 h at room temperature, the solution was poured into water, filtered, and the crude product was purified through silica gel column to yield as a yellow solid of 4.7 g (50%). MALDI-TOF MS: 931.3, calcd for $C_{48}H_{53}Br_2NO_2S_3$: 931.9 ^{1}H NMR (400 MHz, $CDCl_3$, δ, ppm): 7.30 (s, 3H, ArH), 7.05−7.04 (m, 5H, ArH), 6.99 (d, J = 4 Hz, 2H, ArH), 6.94 (d, J = 4 Hz, 2H, ArH), 6.92 (d, J = 4 Hz, 2H, ArH), 6.85−6.83 (m, 5H, ArH), 3.77−3.83 (q, 4H, OCH_2), 1.72 (m, 2H, $CHCH_2$), 1.54−1.32 (m, 16H, CH_2), 0.90−0.96 (m,12H, CH_3). ^{13}C NMR (100 MHz, $CDCl_3$, δ, ppm): 138.327, 135.234,130.903, 130.718, 127.499, 127.063, 126.987, 124.411, 122.688, 120.688, 120.092, 115.472, 113.089, 111.744, 39.635, 30.728, 29.292, 24.060, 23.247, 14.294, 11.334. Anal. Calcd for $C_{47}H_{51}Br_2NO_2S_3$: C, 61.50; H, 5.60; N, 1.53, S, 10.48. Found: C, 61.69; H, 5.55; N, 1.50; S: 10.40.

PT5TPA. Under the protection of argon atmosphere, 0.5 mmol of monomer **5** was put into a two-neck flask. Then 12 mL of degassed toluene and 0.5 mmol of 5,5′-bis(trimethylstannyl)-2,2′-bithiophene were added to the mixture. The solution was flushed with argon for 10 min, and then 25 mg of $Pd(PPh_3)_4$ was added. After another flushing with argon for 20 min, the reactant was heated to reflux for 24 h. Then the reactant was cooled to room temperature and the polymer was precipitated by adding 200 mL of methanol, filtered through a Soxhlet thimble, and then subjected to Soxhlet extraction with methanol, hexane, and chloroform. The polymer was recovered as solid from the chloroform fraction by rotary evaporation. The solid was dried under vacuum for 12 h to get **PT5TPA**.The yield of the polymerization reaction was about 60%. GPC: M_n = 180.9 kg·mol^{-1}, M_w/M_n = 3.2. ^{1}H NMR (400 MHz, $CDCl_3$, δ, ppm): 7.30−6.50 (br, 23H, ArH), 3.86 (br, 4H), 4.87 (s, 2H), 2.26(s, 2H), 1.58−1.02 (m, 40H), 0.89−0.83 (m, 18H). Anal. Calcd for $C_{55}H_{57}NO_2S_5$: C, 71.47; H, 6.21; N, 1.51, S, 17.34. Found: C, 71.38; H, 6.25; N, 1.54; S: 17.41.

■ ASSOCIATED CONTENT

Ⓢ Supporting Information

Figures showing ^{1}H NMR spectra of compound **3, 4**, and **5**, TGA plots, X-ray diffraction pattern, DSC thermogram, and hole mobility measurement of **PT5TPA**. This material is available free of charge via the Internet at http://pubs.acs.org.

■ AUTHOR INFORMATION

Corresponding Author

*E-mail: liyf@iccas.ac.cn.

■ ACKNOWLEDGMENTS

This work was supported by NSFC (Grants No. 20874106, 20821120293, 50933003, 21021091 and 51103164), The Ministry of Science and Technology of China, and the Chinese Academy of Sciences. The authors thank Dr. Hua Geng for the help of the molecular simulation.

■ REFERENCES

(1) Chen, J.; Cao, Y. *Acc. Chem. Res.* **2009**, *42*, 1709.
(2) Cheng, Y.-J.; Yang, S.-H.; Hsu, C.-S. *Chem. Rev.* **2009**, *109*, 5868.
(3) He, Y.; Li, Y. *Phys. Chem. Chem. Phys.* **2011**, *13*, 1970.
(4) (a) He, Y.; Chen, H.-Y.; Hou, J.; Li, Y. *J. Am. Chem. Soc.* **2010**, *132*, 1377. (b) Zhao, G. J.; He, Y. J.; Li, Y. F. *Adv. Mater.* **2010**, *22*, 4355−4358.
(5) Yu, G.; Gao, J.; Hummelen, J. C.; Wudl, F.; Heeger, A. J. *Science* **1995**, *270*, 1789.
(6) Thompson, B. C.; Fréchet, J. M. J. *Angew. Chem., Int. Ed.* **2008**, *47*, 58.
(7) Nagarjuna, G.; Yurt, S.; Jadhav, K. G.; Venkataraman, D. *Macromolecules* **2010**, *43*, 8045.
(8) Grenier, C. R. G.; George, S. J.; Joncheray, T. J.; Meijer, E. W.; Reynolds, J. R. *J. Am. Chem. Soc.* **2007**, *129*, 10694.
(9) Perepichka, I. F.; Perepichka, D. F.; Meng, H.; Wudl, F. *Adv. Mater.* **2005**, *17*, 2281.
(10) (a) Ong, B. S.; Wu, Y.; Liu, P.; Gardner, S. *J. Am. Chem. Soc.* **2004**, *126*, 3378. (b) Ong, B. S.; Wu, Y.; Li, Y.; Liu, P.; Pan, H. *Chem.—Eur. J.* **2008**, *14*, 4766. (c) Li, J.; Tan, H.-S.; Chen, Z.-K.; Goh, W.-P.; Wong, H.-K.; Ong, K.-H.; Liu, W.; Li, C. M.; Ong, B. S.

Macromolecules **2011**, *44*, 690. (d) Li, Y. F.; Zou, Y. P. *Adv. Mater.* **2008**, *20*, 2952.
(11) (a) Sugiyasu, K.; Song, C.; Swager, T. M. *Macromolecules* **2006**, *39*, 5598. (b) Wu, P.-T.; Xin, H.; Kim, F. S.; Ren, G.; Jenekhe, S. A. *Macromolecules* **2009**, *42*, 8817. (c) Miyanishi, S.; Tajima, K.; Hashimoto, K. *Macromolecules* **2009**, *42*, 1610. (d) Li, H.; Sundararaman, A.; Pakkirisamy, T.; Venkatasubbaiah, K.; Schödel, F.; Jäkle, F. *Macromolecules* **2010**, *44*, 95. (e) Rieger, R.; Beckmann, D.; Pisula, W.; Kastler, M.; Müllen, K. *Macromolecules* **2010**, *43*, 6264. Liu, P.; Wu, Y.; Pan, H.; Ong, B. S.; Zhu, S. *Macromolecules* **2010**, *43*, 6368. (f) Liang, Y.; Xiao, S.; Feng, D.; Yu, L. *J. Phys. Chem. C* **2008**, *112*, 7866.
(12) (a) Thompson, B. C.; Kim, B. J.; Kavulak, D. F.; Sivula, K.; Mauldin, C.; Fréchet, J. M. J. *Macromolecules* **2007**, *40*, 7425. (b) Hou, J. H.; Chen, T. L.; Zhang, S. Q.; Huo, L. J.; Sista, S.; Yang, Y. *Macromolecules* **2009**, *42*, 9217.
(13) Ma, W.; Yang, C.; Gong, X.; Lee, K.; Heeger, A. J. *Adv. Funct. Mater.* **2005**, *15*, 1617.
(14) Li, G.; Shrotriya, V.; Huang, J.; Yao, Y.; Moriarty, T.; Emery, K.; Yang, Y. *Nat. Mater.* **2005**, *4*, 864.
(15) (a) Hou, J.; Tan, Z. a.; Yan, Y.; He, Y.; Yang, C.; Li, Y. *J. Am. Chem. Soc.* **2006**, *128*, 4911. (b) Hou, J. H.; Yang, C. H.; He, C.; Li, Y. F. *Chem. Commun* **2006**, 871−873. (c) Hou, J. H.; Huo, L. J.; He, C.; Yang, C. H.; Li, Y. F. *Macromolecules* **2006**, *39*, 594−603. (d) Zhou, E. J.; Tan, Z. A.; Huo, L. J.; He, Y. J.; Yang, C. H.; Li, Y. F. *J. Phys. Chem. B.* **2006**, *110*, 26062−26067.
(16) (a) Zou, Y.; Sang, G.; Wu, W.; Liu, Y.; Li, Y. *Synth. Met.* **2009**, *159*, 182. (b) Wang, Y.; Zhou, E.; Liu, Y.; Xi, H.; Ye, S.; Wu, W.; Guo, Y.; Di, C.-a.; Sun, Y.; Yu, G.; Li, Y. *Chem. Mater.* **2007**, *19*, 3361. (c) Zou, Y.; Wu, W.; Sang, G.; Yang, Y.; Liu, Y.; Li, Y. *Macromolecules* **2007**, *40*, 7231−7237.
(17) (a) Wagner, K.; Crowe, L. L.; Wagner, P.; Gambhir, S.; Partridge, A. C.; Earles, J. C.; Clarke, T. M.; Gordon, K. C.; Officer, D. L. *Macromolecules* **2010**, *43*, 3817. (b) Wang, H.-J.; Chan, L.-H.; Chen, C.-P.; Lin, S.-L.; Lee, R.-H.; Jeng, R.-J. *Polymer* **2011**, *52*, 326. (c) Saini, G.; Jacob, J. *Polym. Int.* **2011**, *60*, 1010. (d) Park, J. W.; Lee, D. H.; Chung, D. S.; Kang, D.-M.; Kim, Y.-H.; Park, C. E.; Kwon, S.-K. *Macromolecules* **2010**, *43*, 2118. (e) Wagner, K.; Crowe, L. L.; Wagner, P.; Gambhir, S.; Partridge, A. C.; Earles, J. C.; Clarke, T. M.; Gordon, K. C.; Officer, D. L. *Macromolecules* **2010**, *43*, 3817. (f) Yu, C.-Y.; Ko, B.-T.; Ting, C.; Chen, C.-P. *Sol. Energy Mater. Sol. Cells* **2009**, *93*, 613.
(18) Sun, H. *J. Phys. Chem. B* **1998**, *102*, 7338.
(19) Bhattacharya, A. K.; Thyagarajan, G. *Chem. Rev.* **1981**, *81*, 415.
(20) Wadsworth, W. S.; Emmons, W. D. *J. Am. Chem. Soc.* **1961**, *83*, 1733.
(21) Carsten, B.; He, F.; Son, H. J.; Xu, T.; Yu, L. *Chem. Rev.* **2011**, *111*, 1493.
(22) (a) Zhang, Z.-G.; Zhang, K.-L.; Liu, G.; Zhu, C.-X.; Neoh, K.-G.; Kang, E.-T. *Macromolecules* **2009**, *42*, 3104. (b) Zhang, Z.-G.; Liu, Y.-L.; Yang, Y.; Hou, K.; Peng, B.; Zhao, G.; Zhang, M.; Guo, X.; Kang, E.-T.; Li, Y. *Macromolecules* **2010**, *43*, 9376.
(23) Sun, Q.; Wang, H.; Yang, C.; Li, Y. *J. Mater. Chem.* **2003**, *13*, 800.
(24) Tsai, J.-H.; Lee, W.-Y.; Chen, W.-C.; Yu, C.-Y.; Hwang, G.-W.; Ting, C. *Chem. Mater.* **2010**, *22*, 3290.
(25) Cunningham, D. D.; Laguren-Davidson, L.; Mark, H. B.; Van Pham, C.; Zimmer, H. *J. Chem. Soc., Chem. Commun* **1987**, 1021.
(26) Kotani, S.; Shiina, K.; Sonogashira, K. *J. Organomet. Chem.* **1992**, *429*, 403.
(27) Tang, R.; Tan, Z. a.; Li, Y.; Xi, F. *Chem. Mater.* **2006**, *18*, 1053.